Q. J. R. Meteorol. Soc. (2004), **130**, pp. 1–20

Using mesocale model winds for correcting wind-drift errors in radar estimates of surface rainfall

By MARION P. MITTERMAIER* , ROBIN J. HOGAN and ANTHONY J. ILLINGWORTH

Department of Meteorology, University of Reading, UK

Accepted Revision 26 January 2004

Summary

For operational radars at middle and high latitudes even the lowest beam of a scan sequence may be above the melting layer for a considerable proportion of the total range. This means that surface rainfall estimates are inferred from measurements made in the snow and ice. Snow and ice are more susceptible to wind-drift than rain because of the low fall speed of around 1 m s^{-1}. Sampling these wind-induced fall streak patterns results in a displacement of the radar-rainfall field when compared to ground measurements. To date wind-drift corrections have only been attempted in the rain, but corrections of around 2 km are generally smaller than the resolution of the grid on which the rainfall field is reported. Observational evidence from this study shows fall streaks in the snow can lead to displacements of the order of 10–20 km, a significant effect, especially in colder climates and seasons.

In this paper a method for calculating and applying a wind-drift correction between the top of the fall streak and the bright band height is presented. The forecast wind profile from the mesoscale version of the UK Met Office Unified Model (UM) is used to calculate the vertical shear of the horizontal wind. We assume the shear and the fall speed in the layer are constant. Results show that the method is able to reproduce observed displacements from high-resolution radar data in the range-height plane. Assessing the effect of applying the method in plan view shows an improvement in the placement of rainfall at the ground, reflected by an increase in the calculated skill scores. The displacement can be corrected to within 20%. This also shows that whereas wind-drift corrections in the rain have been found to be insignificant, corrections in the snow are not. Applying a wind-drift correction also appears to reduce the variability of vertical profiles of reflectivity (VPR) when they are extracted along a fall-streak path, and lead to a smaller reflectivity lapse rate locally. This would suggest that at least part of the reported variability in VPRs is due to wind effects.

Keywords: radar vertical profile of reflectivity shear fall streak wind drift

1. Introduction

Operational radars around the world share a common objective in producing as accurate an estimate of the spatial distribution of precipitation as possible. There are several errors associated with radar-rainfall estimation (e.g. Joss and Waldvogel 1990), and it is acknowledged that the largest source of error is associated with the observed variability of vertical profiles of reflectivity (VPR). Most VPR correction schemes assume that any correction to the reflectivity observed aloft applies to the rainfall rate on the ground below this point, but in reality any wind will cause the position of the precipitation on the ground to be displaced. At middle and high latitudes the radar beam will frequently be sampling the ice. Because the terminal velocity of ice is so much lower than that of rain drops, the ice will be particularly prone to "wind drift" problems. The combination of uncertainty over the VPR correction in the ice above the bright band and the unknown wind-drift lead Fabry *et al.* (1992) to suggest that at moderate ranges once the radar beam is in the ice any attempt to estimate precipitation rates at the ground is "futile".

Marshall (1953) explained the parabolic shape of vertical fall streaks as revealed in radar range-height-indicator (RHI) scans in terms of ice particles falling with constant terminal velocity through a region of constant wind shear, with the pattern itself moving horizontally with the speed of the wind at the height of the generating level. More recently Yuter and Houze (1997) report on observed fall streaks in the rain during TOGA COARE

* Corresponding author: Department of Meteorology, University of Reading, Earley Gate, P.O. Box 243, Reading, Berkshire, RG6 6BB, UK.

(Tropical Oceans Global Atmosphere Coupled Ocean-Atmosphere Response Experiment) that extended downwards from the melting layer but typically not reaching the ground. They also observed fall streaks at different spatial and temporal scales using a vertically pointing S-band radar during the Mesoscale Alpine Programme (MAP)(Yuter and Houze, 2003).

Fabry (1993) suggested that the shape of the fall steak and its displacement as the particles fell from the level of one plan-position-indicator (PPI) scan to a lower PPI could be used to infer the vertical profile of wind, and showed examples where the wind could at best be estimated to about 2.5 m s^{-1}. In this paper we suggest an inverse approach, whereby the profiles of vertical winds held in a mesoscale forecast model are used to correct for wind-drift in the ice. At this point it is important to outline two distinct

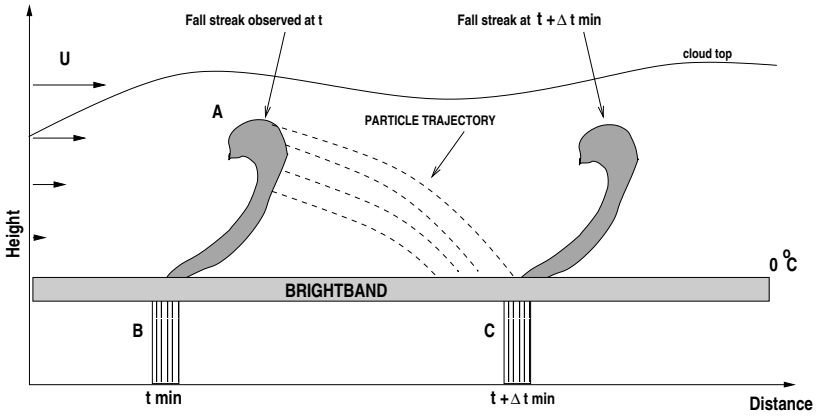

Figure 1. Schematic delineating two distinct problems: To know the rain falling at time t at B, originating from the lowest available elevation radar observation made at t at A, we need to know the fall streak geometry to diagnose the position of the rain (i.e. need to know the wind shear). To know the rain falling at $t + \Delta t$ at location C from the radar observation made at t at A, the position of the rain must be forecast, and includes an advection component.

scenarios, referring to Fig. 1. The first can be described as a diagnostic scenario where we wish to determine where the rain falls at the time of the radar observation. In this case the shape of the fall streak must be determined. This represents the A to B situation in Fig. 1. On the other hand we have a predictive scenario where we wish to predict where the echo observed at location A will fall to ground at some point in the future (typically around 30 minutes if A is 2 km above the melting layer). In this case the trajectory of the individual ice particles must be followed, to reach point C.

It must therefore be stressed that wind-drift errors are caused both by wind shear (as exhibited by the shape of the fall streaks in an RHI) and advection (wind speed multiplied by the time needed for an ice particle to fall from that height to the freezing level, as required for PPIs). Whether the displacements that result from shear and advection go in the same or opposite directions depends on the sign of the shear. RHIs are useful in judging if model winds are sufficiently accurate for explaining the shape of the fall streaks. Operational radars scan in PPI mode so if the lowest observed echo is at height A in Fig. 1 we have two possible approaches of calculating surface rainfall estimates, at B or subsequently at C.

When considering a diagnostic scenario, it is also worth noting that rain gauges, traditionally considered as "ground truth", are also prone to wind effects and turbulence (e.g. Duchon and Essenberg, 2001). The advection distances for rain are small. Harrold *et al.* (1974) found an improvement if the rain was moved with a wind speed es-

timated from two anemometers and a nearby radiosonde ascent. Typical movements were about 1–2 km, as the rain fell at an assumed velocity of 5 m s^{-1} to ground from the height of the radar beam (500 m). Dalezios and Kouwen (1990) found similar distances for wind-drift of the rain. Although such movements are important for gauge calibrations, they are less significant for an operational radar which produces rainfall estimates with a resolution of 1–2 km for use in hydrology. Carruthers and Choularton (1983) present results on the effect of wind-drift on low-level orographic enhancement through the seeder-feeder mechanism. The position of the maximum enhancement is moved downwind and the total and maximum enhancment are reduced for short hills. Collier (1999) also studied how accuracy at different horizontal resolutions was affected by wind drift and suggested that the wind profile type was important in determining the error. Fabry *et al.* (1994) concluded that wind-drift in rain was unimportant for resolutions greater than 5 km. At mid- and higher latitudes the "wind-drift" effect is most important for ice precipitation. If we consider ice which is being detected by the radar 2 km above the bright band and is falling at 1 m s^{-1}, then the displacement can easily become 20–40 km; such a distance is now very significant in hydrology.

The UK state-of-the-art VPR correction scheme (Kitchen *et al.*, 1994) uses a standard vertical profile where the bright band depth is 700 m, and the peak is 350 m below the top which is set to the height where the model wet-bulb temperature T_w is 0°C. The magnitude of the high resolution profile is then scaled to produce the observed reflectivity when the profile is multiplied by the appropriate radar beam width, and the best estimate of the rain at the ground is read off from the scaled profile. This paper extends this philosophy of using the model temperature to fix the bright band height to the use of the model winds to predict wind drift.

Figure 2 shows a RHI scan of nimbostratus with fall streaks on 18 August 2000 at 13:40 UT. Regions of rain and ice, the vertical wind profile, the freezing level (FL) and dotted lines for two vertical cross sections are indicated. For radar-rainfall estimation the

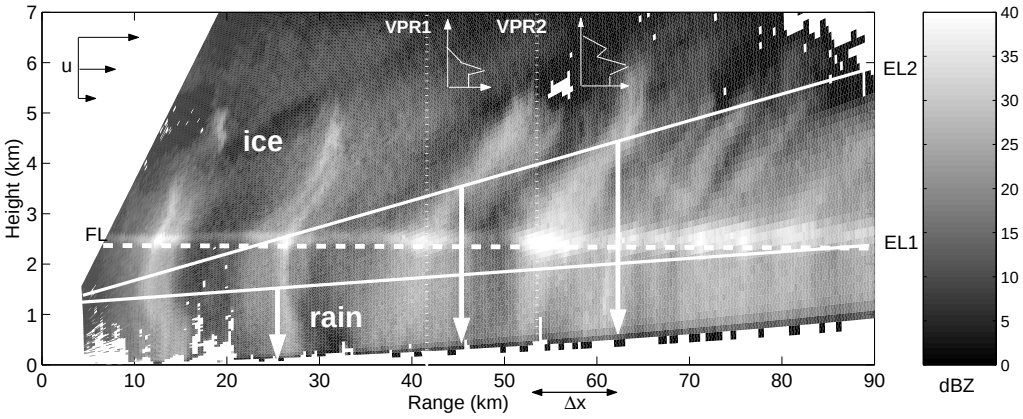

Figure 2. RHI scan for 13:40 UT on 18 August 2000 measured by the 10 cm radar at Chilbolton, southern England, showing fall streaks and how radar beams EL 1 and EL 2 intersect the freezing level (FL) and the fall streaks at different ranges. Downward arrows indicate the surface placement of radar estimates. A displacement error is shown as Δx. Also shown are idealised VPRs extracted at two locations, VPR 1 and VPR 2.

ideal case would be when the lowest elevation beam samples in the rain, never intersecting the bright band within the maximum radar range, like EL 1. Now suppose EL 2 is the lowest beam, with a bright band near the ground. Then the beam would be sampling in

the ice at most ranges. With the presence of shear in the vertical wind profile, sampling at the radar beam height will lead to progressively larger discrepancies between the range where the radar measures and where it is raining at the ground, as shown by the arrows. Furthermore, the presence of fall streaks leads to different VPR shapes. VPR 1 is an idealised profile more typical of stratiform rain with a rapid decrease in the reflectivity above the bright band. VPR 2 on the other hand would indicate an increase in the reflectivity higher up, as the top of the next fall streak element is intersected by the radar beam. We therefore hypothesise that some of the observed variability in VPRs is due to wind effects.

Panagi *et al.* (2001) report on comparisons between wind profiler data from various locations around the UK and Europe and Met Office Unified Model (UM) wind profiles. Regardless of whether the data were assimilated or not most of the profiles showed that the *rms* errors below 4 km height are less than 1 m s^{-1}. Turton *et al.* (1994) state that the model-derived wind profiles are preferable to radiosonde profiles once 3 hours has elapsed since the sonde launch. Sondes are launched only every 6 or 12 hours at a few locations, so we conclude that the model winds which are available at every grid point every hour are the best source of wind data.

In this paper we explore a new radar-model synergy, by proposing the use of UM mesoscale model forecast winds to correct for wind drift of falling ice and snow above the freezing level, addressing both diagnostic and predictive cases. First, in Section 2 an equation for calculating displacements using the model winds is presented. A comparison between model and radar-derived wind profiles is given in Section 3 to establish whether the model winds are indeed good enough to use. In Section 4 the magnitude of observed displacements in RHIs are investigated. The sensitivity for errors in fall speed and generating level height is discussed next in Section 5. Sections 6 and 7 then present two case studies where the method is applied in the vertical plane and plan view. Section 8 outlines potential implications for the variability of VPRs. A modified method and a discussion on errors for the operational implementation of a predictive scenario are given next in Section 9. Conclusions follow in Section 10.

2. A theoretical model of fall streak geometry

To devise a method, the following assumptions, adapted from those made by Dalezios and Kouwen (1990), are made:

i. The fall speed w of the ice, is *constant*.
ii. The wind profile is *linear* between the generating level height and the bright band, implying *constant* vertical shear for the u- and v- components.

We take the approach that natural uncertainties in the fall speed and generating level height do not justify a more complex model. A schematic introducing the fall streak geometry is given in Fig. 3. We can consider the two wind components independently. First consider the effect of wind drift in the zonal (x) direction. The vertical shear of the horizontal wind, S_x is calculated for the layer between two reference heights, the freezing level (FL) ($h = 0$) and a fall streak source region or generating height, h_t. The height that precipitation has fallen from h_t is denoted as h_f, with a corresponding zonal displacement x_f.

Similar to the approach of Marshall (1953), the time to fall a distance h_f from h_t is h_f/w. In this time the air at the top of the fall streak has moved zonally a distance $(u_t\ h_f)/w$ where u_t is the wind at the generating level height. As the zonal shear S_x is

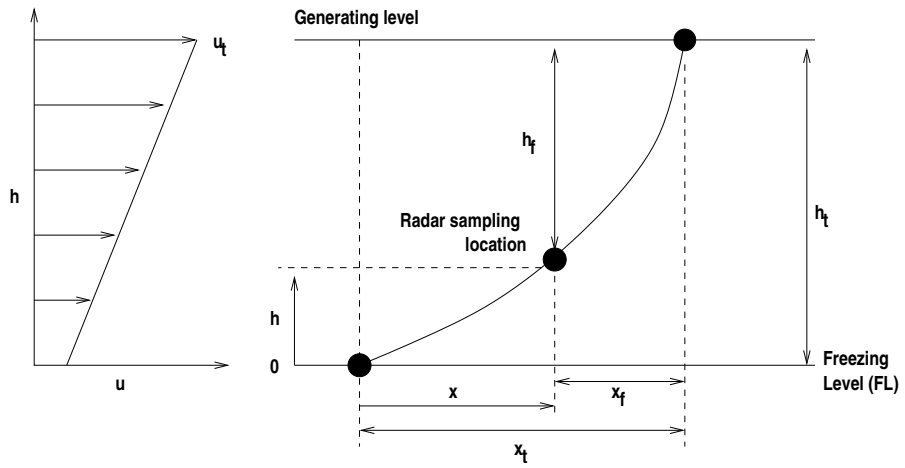

Figure 3. Fall streak geometry showing the linear wind profile that is assumed in height, giving constant shear. The height of the generating level is denoted as h_t, which is the where the maximum horizontal displacement x_t occurs. At any given height, h relative to the freezing level (FL, $h = 0$), the distance x can be calculated.

assumed constant, the horizontal displacement of a falling ice particle is determined by the average zonal velocity that it experiences as it falls a distance h_f, which is

$$u_t - \frac{S_x\, h_f}{2}. \tag{1}$$

Therefore the zonal displacement relative to the new position of the source region at the generating level is

$$x_f \;=\; \frac{S_x\, {h_f}^2}{2\, w}, \tag{2}$$

showing that the shear controls the shape of the fall streak and the absolute horizontal velocity is irrelevant. From the figure, $h = h_t - h_f$ and $x = x_t - x_f$. The maximum displacement occurs when the radar samples at the generating level height, where $h_f = 0$ so that $h_t = h$:

$$x_t \;=\; \frac{S_x\, {h_t}^2}{2\, w}, \tag{3}$$

and to know the displacement of precipitation sampled at any height h between h_t and $h = 0$, we substitute x and h to get

$$x \;=\; \frac{S_x}{w}\,\left(h\, h_t - \frac{h^2}{2}\right); \tag{4}$$

similarly for meridional displacement y with shear S_y. Given the assumptions, the displacements, x and y at any given height above the freezing level can then be calculated using Eq. 4, indicating a parabolic fall streak shape. The magnitude of the displacement scales linearly with the shear S and inversely with fall speed, w.

Operationally, direct measurements of the fall speed w are not available. Similarly the height of the generating level will not be directly observed due to the way in which operational radars scan. Using the radar data itself might seem like the optimal solution, but determining the generating level objectively, even when RHI data are available, is difficult.

It would be straight forward to then make a small further correction for the orientation of fall streaks in the rain but the purpose here is to evaluate the ability to correct for wind-drift in the ice.

3. Justification of use of model winds and temperatures

In order to use the model winds we first need to ensure that they are accurate enough for our purposes. Turton *et al.* (1994) and Panagi *et al.* (2001) have reported on validation of model winds using radiosondes and wind profilers. Here, wind profiles derived from Doppler radar are used as an independent source for comparison.

(*a*) *Comparison to radar-derived Doppler wind profiles*

The radar data were collected using the 3 GHz radar situated at Chilbolton in southern England (51.14°N and 1.44°W)(see Goddard *et al.*, 1994). The large 25 m antenna affords a beam width of 0.28°. Both RHI and PPI data at 300 m range resolution were used. Vertical sampling occurs at 0.1–0.2° elevation steps, between 0–30° elevation. PPIs have 0.25° resolution in azimuth. An earth curvature correction was applied. Nine events between March 1999 and November 2000 were studied.

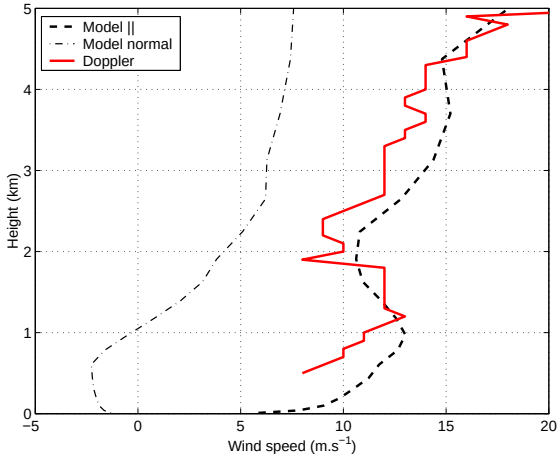

Figure 4. Wind profiles derived from the horizontal component of RHI Doppler winds for 13:40 UT on 18 August 2000 and the hourly model forecast. The plane-perpendicular model wind profile is also shown.

For the current work, single-column mesoscale model wind profiles from the 2000 version of the UM (12 km horizontal grid spacing) for the Chilbolton grid reference were compared to vertical profiles of wind derived from the horizontal component of the radial Doppler wind. The radar winds were averaged into 100 m bins in the vertical and over the entire radar range of 90 km. For further information on the UM the reader is referred to Cullen (1993). Fig. 4 shows such a comparison for one RHI scan with the along-RHI component of the hourly (t+2h) model wind forecast. Forecasts are in the t+0h to t+5h range. Despite the discrepancies in vertical and temporal resolution between the radar and model data, the comparison is remarkably good. The plane-perpendicular profile is also shown for reference.

The comparison can be taken one step further and several scans within the same hour can be evaluated, and also other hourly forecasts on other days. Figure 5 shows

the comparison of the mean layer winds for 34 scans, spanning 6 days between August and November 2000, and representing 10 hourly forecasts. As the aim is to evaluate the lower-mid-tropospheric winds, the top of the layer was here defined to be the model level closest to 4 km, the bottom being the model level closest to the freezing level. The mean layer wind calculated from Fig. 4 is but one of the data points on this graph. This suggests a good correspondence between model and radar-measured winds for a spectrum of weather systems, with a correlation of 0.94, but a mean error of 2.67 m s^{-1} which is larger than the 1 m s^{-1} quoted by Panagi *et al.*, but is for a small sample of radar data whereas the 1 m s^{-1} was determined from a year's model output fields. It can therefore be concluded that the model winds with errors of 1 m s^{-1} are good enough to use for wind-drift correction of radar data. Furthermore, the last assumption in the method can now be added:

iii. Model wind profiles are sufficient and accurate enough to use.

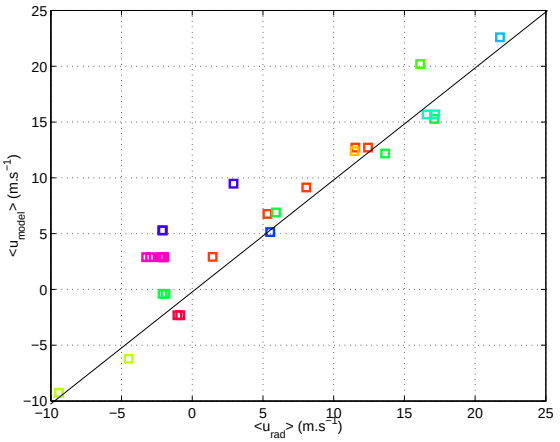

Figure 5. Plot of the mean layer winds as determined from the model, against the mean layer wind calculated from Doppler velocity data. A 1:1 line has been added for reference. The correlation is 0.94.

(*b*) *A model climatology of wind speed and shear*

The 34 RHI scans included in this study are useful for conceptualization, testing and validation. But the data set is insufficient to, say, determine the range of displacements and the conditions that lead to them. This is because of the requirement that for RHIs, the radar should sample along the mean wind direction and there should be little variation in wind direction with height. To capture this range of displacements a two-and-a-half year time series of UM single column forecasts for the Chilbolton grid reference (mid-1999 to end 2001) was analysed to determine the distributions of wind speed and shear. The results are shown in Fig. 6, obtained by considering the same layer between the freezing level and the model level nearest 4 km.

Ninety percent of the data have a shear between 6×10^{-4} and 5.4×10^{-3} s^{-1}, and average layer winds are between 3 and 24.5 m s^{-1}, with a mean of 12 m s^{-1}. From a correction point of view it is useful to know whether the shear scales with the magnitude of the wind. Fig. 7 shows the contoured distribution of wind speed and shear. It shows that there is no clear relationship between the two and that high winds are not a prerequisite for strong shear, with typical values of 5–10 m s^{-1} and 0.002 s^{-1}. So, a layer depth of

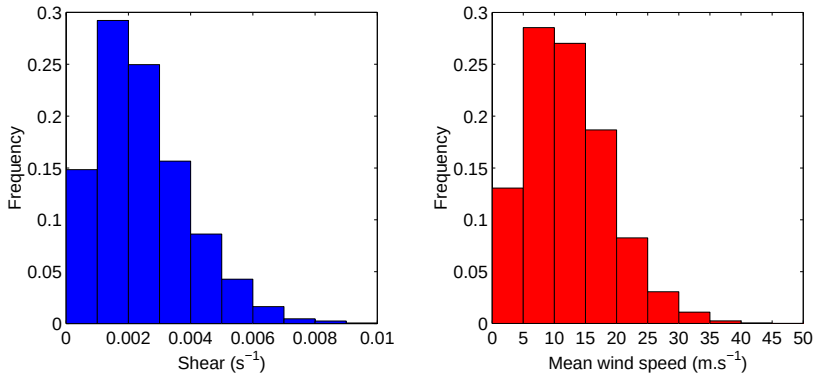

Figure 6. Two-and-a-half year model climatology of shear and mean wind speeds between the freezing level and 4 km.

2.5 km, a shear of 0.002 s^{-1} and a fall speed w of 1 m s^{-1} yields a maximum fall streak displacement of 6.25 km.

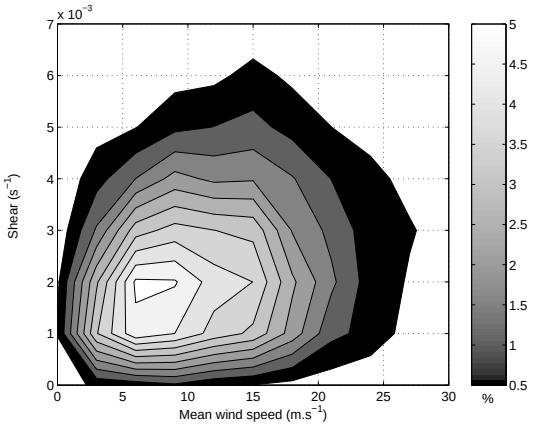

Figure 7. Contoured distribution of mean layer winds and layer shear from the model climatology. Contours are at every 0.5% between 0.5–5%.

(*c*) *Model vertical temperature structure*

Mittermaier and Illingworth (2003) showed that the UM mesoscale forecasts of the vertical temperature structure is good with freezing levels within 147 m for a one-year comparison to vertically-pointing cloud radar data. The study showed that heights can be derived with confidence from the model temperatures.

4. Observed displacements

The slope of fall streaks and displacements can be calculated from RHI data using a radar-only approach by using the concept of lagged correlations in space. The generating level is defined as the height where fall streaks originate, which can be subjectively determined from RHI data, but would not be obvious from operational PPIs. Data series at constant heights are extracted from an RHI, one located in the rain, which is the

reference. The other heights, located in the ice, are spaced 500 m apart. A range of heights is required because if a fall streak exists, it should intersect at least one of these heights, the maximum displacement determined by the convergence of the correlation traces from different heights. For correlation the data series were converted to linear Z space to assist in identifying the fall streak peaks in the ice. This was to increase the difference in magnitude between the reflectivity in the fall streak and the background.

Maximum displacement would be associated with the radar measuring at the top of the fall streak. An example of such correlation traces is given in Fig. 8. The correlations were calculated between a reference series in the rain at 1 km and a sequence at heights from 2.5–5 km in the ice, 500 m apart. In this case the traces converge at a displacement of 22 km at a height of 5 km.

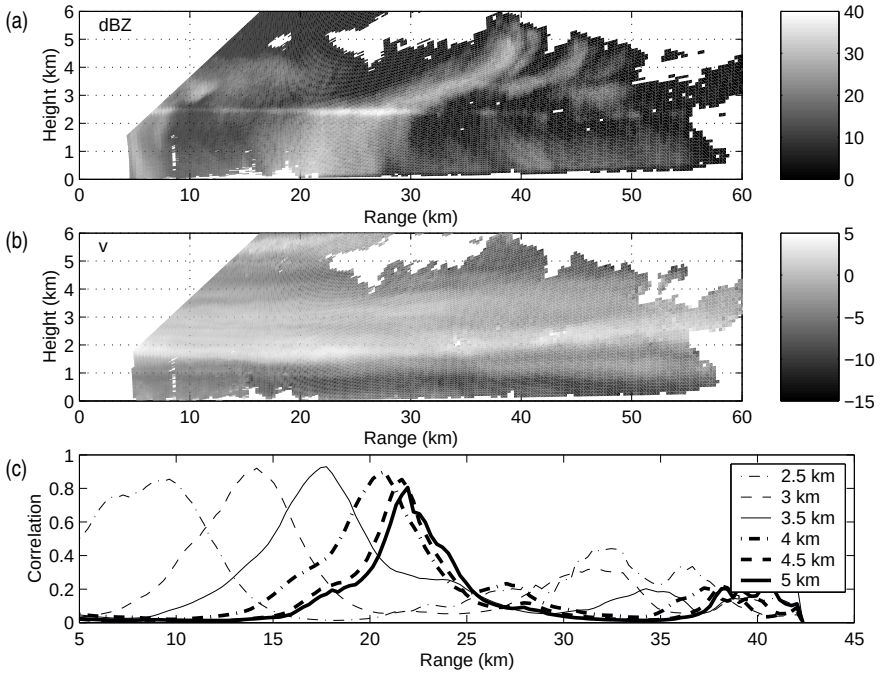

Figure 8. RHI for 13:31 UT on 18 August 2000 showing (a) reflectivity and (b) Doppler winds (m s^{-1}), positive away from the radar. Also shown are distance correlation traces (c), each trace represents the correlation between two constant-height data series, one at 1 km below the bright band and the others heights between 2.5–5 km.

The method does provide an independent quantitative means of calculating radar-only displacements, not affected by the assumptions made in this paper, providing the means for comparison to the model-calculated values discussed in Section 6.

5. Optimum parameters for use in fall streak model

(*a*) *Fall speed*

In Eq. 4, the fall speed is a key parameter. For stratiform rain, the region up to 2 km above the bright band is typically dominated by aggregates of ice and snow. Fall speeds of around 1 m s^{-1} are typical (e.g. Locatelli and Hobbs, 1974). Empirical relationships linking radar reflectivity and fall speed have been derived for rain and snow (e.g. Sauvageot, 1992) but these have been disputed, mainly because the accuracy depends on precipitation type.

The fall speed can also be investigated using the RHI data in an exploratory manner to see how they compare to those quoted in the literature. Displacements can be calculated using the measured shear in the layer from the radial Doppler winds and a range of fall speeds between 0.5–5 m s^{-1}. A variation on the correlation method described in Section 4 can be used to determine the fall speed associated with the peak in the correlation trace.

For this purpose 25 carefully selected RHIs, aligned with the wind, were used. Although this is a small sample it contains reflectivity values ranging between -5 and 30 dBZ at the generating level height. Only two constant-height series were extracted, one below the bright band in the rain, the other at the generating level height. The horizontal displacement of the fall streaks is typically 10–15 km. An example correlation trace is shown in Fig. 9, suggesting a fall speed of 0.95 m s^{-1}. Peaks for the 25 cases are 1.02±0.21 m s^{-1}, suggesting that a constant fall speed of 1 m s^{-1} is appropriate.

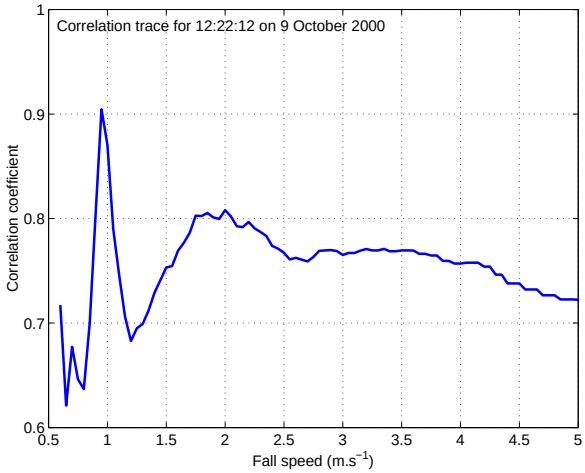

Figure 9. Correlation trace between a series in the rain at 1.8 km and the other at the observed generating level of 4.5 km using a range of fall speeds for the RHI at 12:22 UT on 9 October 2000.

(*b*) *Sensitivity to the height of the generating level*

Knowing the depth of the layer between the generating level and the freezing level is important for establishing the present position (on the ground) of the generated precipitation, but is difficult to determine, even from RHI scans. Some proxy for this height would need to be found that will capture the average behaviour. An analysis of the hourly model wet-bulb temperatures associated with the observed generating level heights for

the scans in this study have a mean of -14.8 ± 1.7°C. The mean observed layer depth calculated from the RHI scans used in this analysis is 2.6 km.

An analysis of the two-and-a-half year model time series described in Section 3(b) gives the mean model layer depth between the -15°C and 0°C wet-bulb temperature isotherm heights as 2.8±0.5 km, representing the seasonal fluctuation. It is remarkable how consistently close the -15°C is to the generating level height but as yet no microphysical reason for this could be established.

6. A case study of fall streaks in the vertical plane

When applying the technique in the vertical plane, the largest difficulty is motion through the plane. Therefore to apply the technique to RHIs, scans must be found where the wind speed can change with height but the direction is constant, i.e. unidirectional speed shear. Therefore we specify that the component of the forecast model wind perpendicular to the RHI must be small (less than half) compared to the magnitude of the plane-parallel wind component, and this must be the case for the entire depth of the layer that the correction is to be applied to. In Fig. 10 one of the four remaining RHIs for 18 August 2000 at 13:40 UT at 25° azimuth that meet the above criteria is shown. A strong bright band with fall streaks is evident. This is a relatively low shear case with the shear calculated from the radar data was 0.0015 s^{-1} and the model shear calculated from a t+2h forecast was 0.0017 s^{-1}. A constant fall speed of 1 m s^{-1} was used. Fall streak geometries and displacements calculated using Eq. 4, based on the height that precipitation has fallen from observed generating level are superimposed as white dashed lines. Displacements of between 7–12 km were calculated for layer depths of 2.9–3.7 km. This corresponds well with the lagged-correlation displacement of 7 km. The shape and displacements are captured well by the calculations, suggesting that the constant fall speed, shear and single-column assumptions are sufficient.

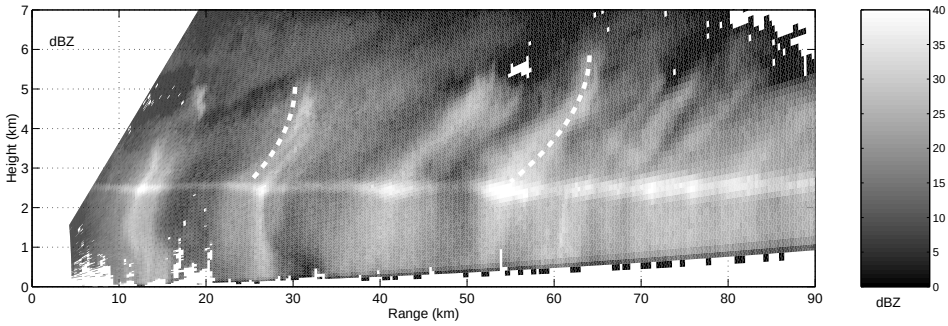

Figure 10. RHI for 18 August 2000 at 13:40 UT at 25° showing clear fall streaks. Fall streak trajectories calculated using Eq. 4 are superimposed.

The two fall streaks were produced using two different generating level heights, with the layer depth 2.9 and 3.7 km. The magnitude of the calculated displacements is dependent on the generating level height which for the RHI data is *a priori* information. From the radar measurements, depending on the reflectivity threshold that is used, a mean generating level height of 5.5 km for the scan seems appropriate.

7. Case study of wind drift in plan view

All operational radars collect data in volume mode, as a sequence of plan-position-indicators (PPI), one of the purposes being the calculation of radar-rainfall estimates. We now consider a PPI in a diagnostic sense, but because we are comparing to another PPI at a different elevation, a small advection correction was still required to get the two PPIs aligned in time (less than 2 minutes, as oppposed to the time delays of the order of 30 minutes referred to in Section 1.) Operationally, PPIs would typically be corrected for in a predictive manner.

The PPI sequences analysed are for 30 March 1999. Prior to May 1999, no UM data were available so the European Centre for Medium Range Forecasting (ECMWF) model forecast for the Chilbolton grid location was used instead. Fig. 11 (a) shows the vertical wind and temperature profiles for 12:00 UT (t+24h) and 13:00 UT (t+25h), and (b) shows the hodograph of the horizontal wind at 12:00 UT. There are no significant changes between the two hourly forecasts.

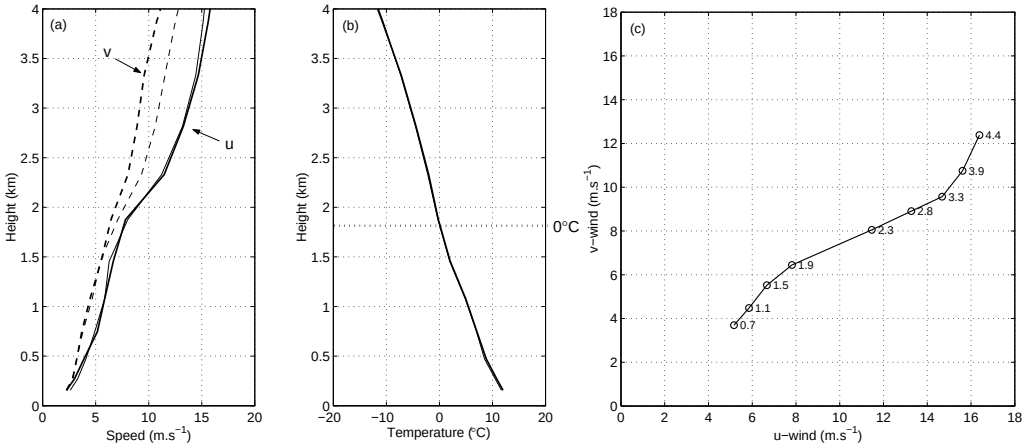

Figure 11. ECMWF wind (a) and temperature (b) profiles for 12:00 UT (t+24h) and 13:00 UT on 30 March 1999 for Chilbolton grid location. The hodograph for 12:00 UT (c) shows that the wind shear is unidirectional.

The freezing level is just below 2 km and the wind speed is increasing with height. The hodograph was approximately unidirectional, so the shear is mostly due to the change in the strength of the wind with height.

Both the radar-only analysis of an RHI as described in Section 4 and applying Eq. 4 gives displacements of ∼23 km when precipitation falls from the generating level. An aspect not addressed thus far is the issue of spatial scales. The UK Met Office produces radar-rainfall fields at three different resolutions. The national composite is at 5 by 5 km, but there are also 2 by 2 km and 1 by 1 km products produced for individual radars, primarily for hydrological applications. One of the main objective besides devising a method for applying a wind-drift correction is determining the magnitude of the correction in relation to the product resolution.

To illustrate the method, and for validation purposes the correction is applied at ranges where 0.5° elevation data are also available below the bright band, in the rain. Figure 12 shows the uncorrected and corrected sector scans at 2.5° elevation on 30 March 1999 at 11:42 UT together with the 0.5° sector scan PPI at 11:44 UT, as 1, 2 and 5 km contoured fields of rain rate, R. Only areas of potential overlap are shown for each field. A

simple VPR slope correction was applied to both uncorrected and corrected 2.5° scans by applying a 3 dB.km^{-1} reflectivity lapse rate as a function of height. This was calculated from the scan itself. A system advection correction to account for the time difference between the scans at the two elevations was also applied. The maximum rain rate was of the order of 1.8 mm h^{-1}. This is therefore a low rain-rate event but for the UK, a rather typical example. The uncorrected 2.5° PPI shows no rain in the area coincident with the 0.5° rain area. After the application of the fall streak (up to 8.7 km) and advection (1.6 km for 102 s scan separation) correction the rain area is now in the same place, especially the position of the closed 1.6 mm h^{-1} contour at 10 km north, 40 km west. The pattern is evident at all spatial resolutions, implying that the correction has made a positive impact at all these scales.

A standard technique for evaluating the positioning of rainfall in precipitation forecasts from models is the use of rain-rate thresholds and binary maps, combined with a contingency table and various skill scores (e.g. Mason, 2003). This approach was applied here to evaluate the effect that the correction has had on the positioning of the rainfall. To compile the contingency table all the pixels for the 0.5° PPI above a pre-determined threshold are set to "1" (else "0"), and similarly for both the uncorrected and corrected 2.5° PPIs. The area of overlap at that rain-rate threshold is then determined, and the pixels counted, depending on whether it is a hit, a miss, a false alarm, or a correct rejection. This is shown in Fig. 13. Two measures derived from a contingency table were used to evaluate the success of the wind-drift correction, the *bias* and the *equitable threat score* (ETS) given in Eqs 5 and 6. The ETS is also known as the Gilbert's skill score. The bias in this context is the ratio of the number of observed occurrences at 2.5° to the number of observed occurrences at 0.5°. A bias of 1 would imply that the correct number of forecasts are made, when compared to the actual observations. The ETS takes the hits that would have occurred purely by chance into account.

The bias and ETS for three PPI sequences on 30 March 1999 of 0.5° and 2.5° including the example in Fig. 12 are plotted as a function of rain-rate thresholds (0.3–1.3 mm h^{-1}) in Fig. 14. Specifically the uncorrected-to-0.5° and the corrected-to-0.5° are plotted for the 1, 2 and 5 km resolution fields.

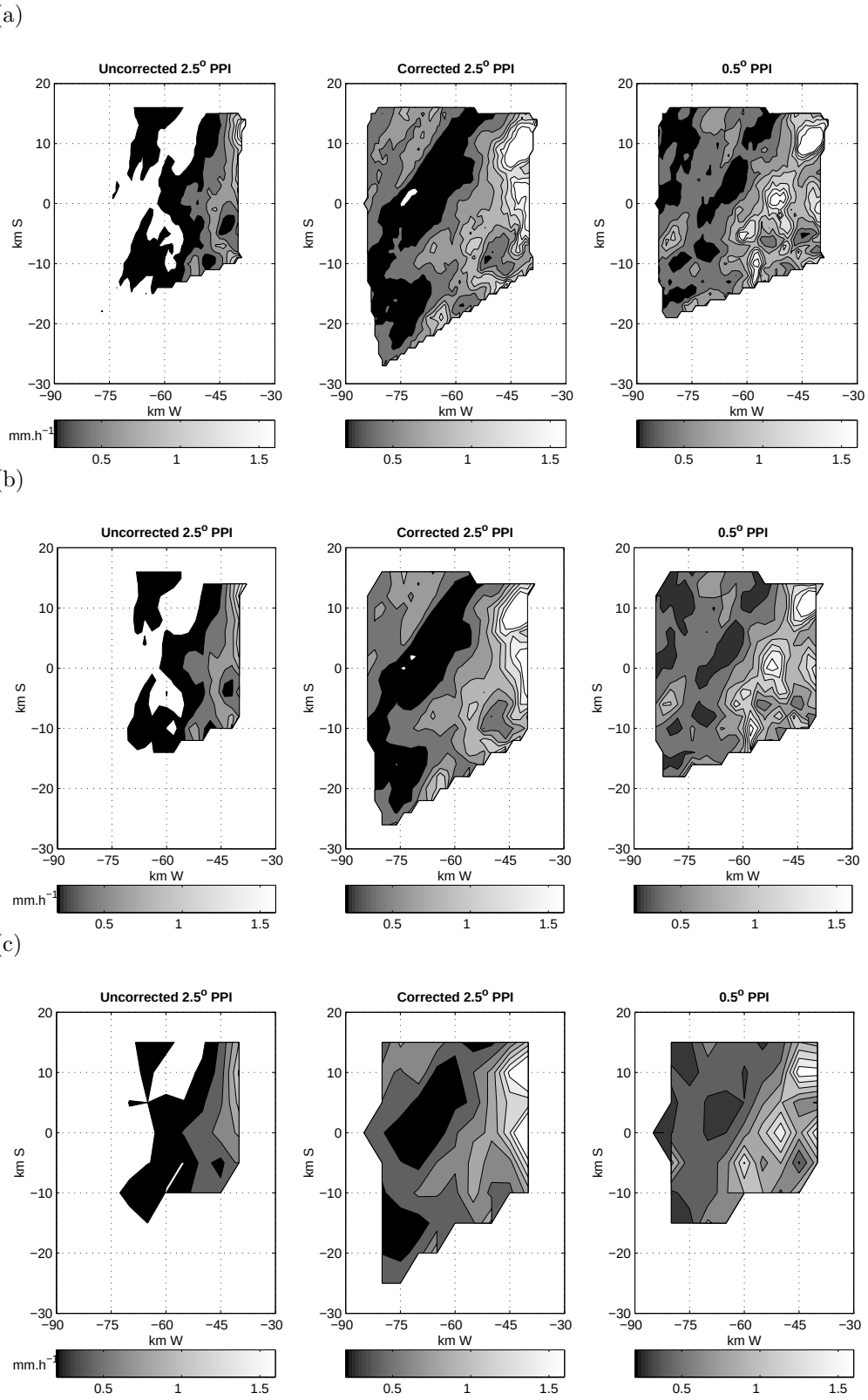

Figure 12. Uncorrected and wind-drift corrected 2.5° PPIs and the 0.5° counterpart as (a) 1 km, (b) 2 km and (c) 5 km averages of rainfall rate. Contour intervals are at 0.2 mm h^{-1} between 0.2–1.6 mm h^{-1}.

		Observed at 0.5deg		
Observed at 2.5deg	EVENT	yes	no	Total
	yes	*a* ("hit")	*b* ("false alarm")	*a + b*
	no	*c* ("miss")	*d* ("correct rejection")	*c + d*
	Total	*a + c*	*b + d*	*a+b+c+d=N*

Figure 13. Schematic of a contingency table showing the meaning of each of the values.

$$B = \frac{a+b}{a+c} \tag{5}$$

$$ETS = \frac{a - \left(\frac{(a+c)(a+b)}{N}\right)}{a+b+c-\left(\frac{(a+c)(a+b)}{N}\right)} \tag{6}$$

(a)

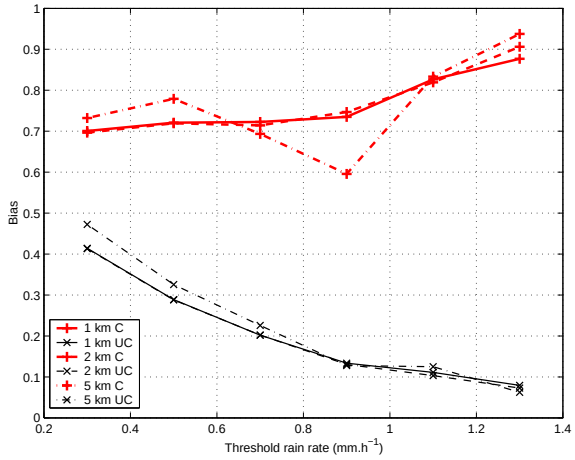

(b)

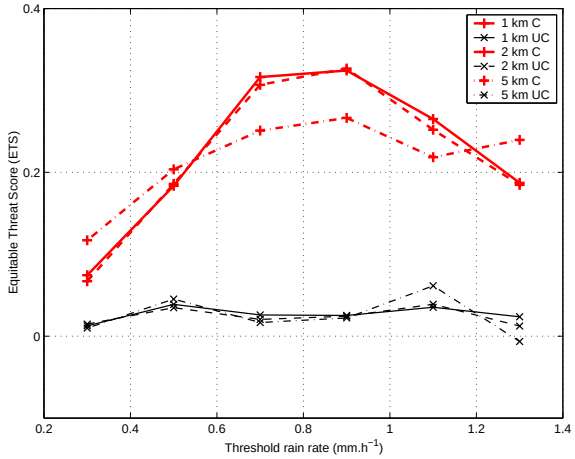

Figure 14. The corrected (C) and uncorrected (UC) bias (a) and equitable threat score (ETS) (b) at all spatial scales and for different rain rate thresholds, from 0.3 to 1.3 mm h^{-1}.

As the bias is always less than 1, there is always an under-estimate in the observed occurrences at 2.5°, both for the uncorrected and corrected fields. The absolute value of the bias is affected by the lapse rate used to correct the VPR. The bias for the corrected field is better (closer to 1) with an improvement in the bias for rain rates

greater 1 mm h^{-1}, which is unusual in the forecast validation context where the skill of predicting more intense events often decreases. The ETS measures the accuracy of the estimate, i.e. how many "hits" are matched. Again the ETS for the corrected field is better at all rain-rate thresholds. This substantiates in a quantitative manner the improvement that can be seen, at all spatial scales.

8. Implications for Vertical Profiles of Reflectivity

Conventionally, VPRs are extracted as truly vertical profiles for the purposes of defining the shape of the VPR and VPR correction. We define a "fall streak profile of reflectivity" or FSPR, which is extracted along a fall-streak path using the model wind shear and the parabolic fall streak geometry model. Figure 15 shows the mean FSPRs and VPRs extracted from four 5 km range intervals from the RHI shown in Fig. 10. To avoid the bright band zone, profiles were calculated between 3.1–5.5 km. We find that a considerable proportion of FSPRs locally exhibit a significantly smaller decrease in reflectivity with height, particularly in the 1–5 km above the bright band, when compared to the more familiar decrease of reflectivity with height of the VPRs. The average VPRs for 40–45 km and 50–55 km (with respect to surface range) are examples as shown in Fig. 2 where the higher reflectivities of the generating level source region are intersected. This can still happen for FSPRs, e.g. for 40–45 km above 5 km, because the generating level was not optimally defined for this interval. Even with coarser vertical resolution (in terms of the number of elevation steps), the behaviour should still be discernible. So long as local averages are taken, differences between FSPRs and VPRs should be apparent. In this case a 5 km horizontal averaging length was used, and it so happened that there were a few clear averaging intervals that coincided with the location of more or less intense rainfall.

Even more important than the mean profiles is the spread or variability because whereas the mean VPR and FSPR for an entire RHI would be equal, the spread is not. This is shown in Fig. 16 where the standard deviation of 200 normalised VPRs and FSPRs (with respect to reflectivity in the rain) in dB is plotted against absolute height, above the bright band, extracted from the RHI shown in Fig. 10. The values for the profiles extracted along the calculated fall streak geometry have lower standard deviations at all heights with differences in the spread of up to 2 dB between the VPRs and FSPRs. The normalised mean profiles are almost identical, as ought to be expected over the entire RHI.

These differences would suggest that some of the observed variability is because the wind effect has not been taken into account. The rapid decrease of reflectivity in the ice is delayed to above the generating level height with FSPRs displaying higher reflectivities.

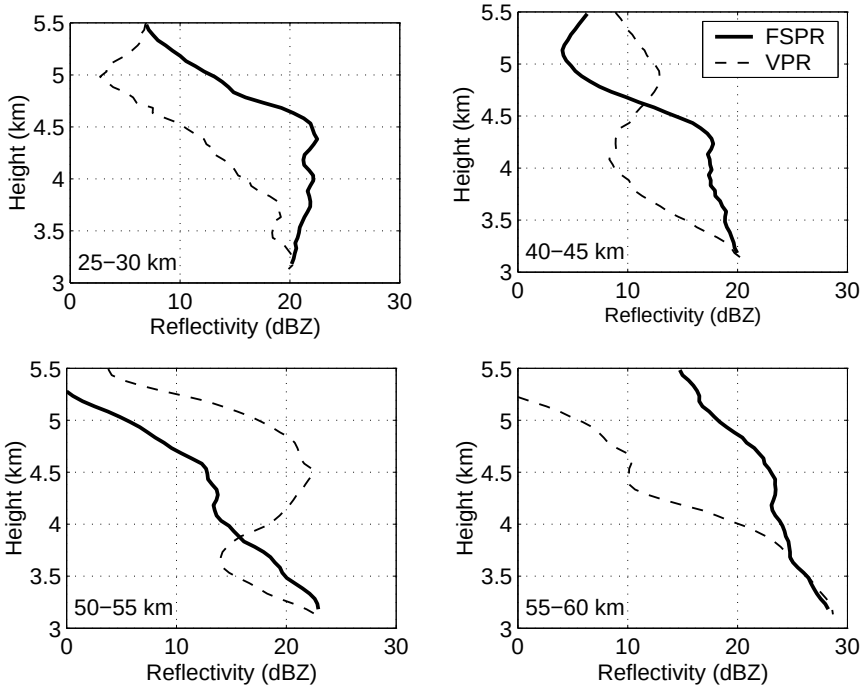

Figure 15. Example of VPRs and FSPRs for 5 km range intervals, for the RHI in Fig. 10 for 18 August 2000, 13:40 UT.

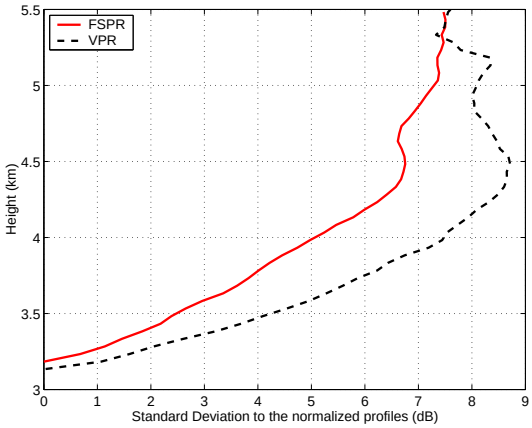

Figure 16. Comparison of the standard deviations of 200 normalised (with respect to reflectivity in the rain) VPRs and FSPRs for the RHI shown in Fig. 10 on 18 August 2000 13:40 UT, plotted against absolute height.

9. Implementing a predictive scheme - operational considerations

In the preceeding sections we have described a method of accurately diagnosing the instantaneous location of the surface rainfall given a measurement in the ice. With regards to the operational implementation of a wind-drift correction, the advection and shear could be dealt with simultaneously by advecting a radar volume of reflectivity Z from the lowest observed PPI at height h using the u and v components of the mesoscale

model wind at that height whilst allowing the volume to descend at a fall speed w. This is computationally an expensive scheme and the uncertainties in w remain, i.e. a more "accurate" implementation does not necessarily yield better results.

(*a*) *A modified formula*

An equation for calculating a relative displacement, based on Eq. 4 can be derived, and is given in Eq. 7. The mean model shear S_x is calculated between the radar beam height h and the melting layer height h_m, and is probably adequate. A displacement x, with respect to the ground can be calculated using

$$x = \frac{1}{w}\left[u_m\,(h - h_m) + \frac{S_x}{2}\,(h - h_m)^2\right], \tag{7}$$

and similarly for y. The shear is calculated as $S_x = (u - u_m) \,/\, (h - h_m)$ where u is the horizontal wind at the radar beam height and u_m the horizontal wind at the freezing level. Again a similar expression could be used for the displacement in the rain using a larger, more appropriate value of w.

(*b*) *Sensitivity of wind drift to fall speed and wind speed errors*

In an operational environment the lowest PPI would be used to predict the position of the rain on the ground. We now examine the expected errors in this prediction when using Eq. 7 if the model winds are known to within 1 m s^{-1} and the terminal ice fall speed to within 20%. In an operational situation the radar beam could be up to 2 km above the bright band and using the model temperature should be known to within 7%. If, from Fig. 6, the mean wind is 10 m s^{-1} and the mean shear is 0.002 s^{-1}, then the wind drift down to the melting layer will be 20 km due to advection with a 20% error and 4 km from shear with a 20% error, assuming that the errors are independent. This leads to an estimated wind-drift of 24 km with a 4.5 km error. For more extreme winds of 20 m s^{-1} the wind-drift would be 40 km due to advection with an unchanged shear correction, leading to a net drift of 40 ± 8 km. To this must be added the drift in the rain. If the melting layer was 2 km above the ground, and the same strong winds extended all the way to the ground, then a further 5 ± 1 km should be added. In summary wind drifts of 20–40 km could occur and the corrections should be accurate to about 20%.

10. Conclusions

Observational evidence shows that vertical shear of the horizontal wind can cause displacements in the positioning of the present surface rainfall derived from radar measurements in the ice of 10–20 km. For predictive calculations, of where the observed radar echo will subsequently reach the ground, advection by the horizontal wind can also be a significant effect. Comparisons of the model wind profiles with the wind profiles derived from the radial Doppler winds show good correspondence, suggesting that using the model winds for a wind-drift correction scheme is feasible.

A method using a single-column wind profile forecast from the UM mesoscale version together with assumptions of a linear wind profile, a constant fall speed and a constant temperature of the generating level has been proposed. It has been shown it can reproduce observed displacements due to vertical shear of the horizontal wind and improve the ground placement of radar-derived precipitation, as indicated by the better bias and skill scores. The use of a constant 1 m s^{-1} fall speed in calculations appears adequate.

Corrections are applied to a layer between the freezing level and a generating level height which coincides with the top of the fall streak. As the generating level may not be directly observed operationally, the -15°C wet-bulb temperature derived from the model was considered for use instead of an observed generating level height. It has been shown that it yields layer depths of the right magnitude so that the height of the -15°C wet-bulb temperature isotherm can be considered an adequate proxy. Calculated displacements are sensitive to this layer depth, which is on average 2.8 km.

Vertical profiles of reflectivity extracted along calculated fall-streak paths (FSPRs) show a lower spread than ordinary VPRs, suggesting that at least some of the variability in the observed VPRs is due to wind effects aloft. Some FSPRs exhibit an almost constant reflectivity with height, more reminiscent of convective profiles. This is significant for VPR correction schemes and calculating local lapse rates of reflectivity in ice, in particular, *when* the VPR correction scheme is applied. More data, perhaps RHIs (with the constraints as described) will need to be collected and analysed to evaluate the effect on VPRs.

We suggest that the predictive method be implemented and tested operationally given that displacements of 20-40 km can occur. For the UK this would involve the application of a wind-drift correction *before* correcting the VPR. The correction should be applied every volume scan, keeping track of the location and time that precipitation takes to reach the freezing level. In such a way precipitation can be allocated to the correct volume scan time. A re-sampling of the field would be required to maintain continuity. Work to this end has been initiated. Implementing a wind-drift correction scheme in a predictive sense will provide a more accurate placement of precipitation before it has fallen to ground, improving quantitative precipitation forecasts.

Acknowledgement

We thank the Met Office and ECMWF for model data and the Radio Communications Research Unit (RCRU) at RAL for the radar data. The authors wish to thank Malcolm Kitchen and Barbara Casati for useful discussions. The work was funded by the Environment Agency through Met Office contract PB/B3567.

References

Carruthers, D.J. and Choularton, T.W. 1983 A model of feeder-seeder mechanism of orographic rain including stratification and wind-drift effects. *Q. J. R. Meteorol. Soc.,* **109** , 575–588.

Collier, C.G. 1999 The impact of wind drift on the utility of very high spatial resolution radar data over urban areas. *Phys. Chem. Earth. Part B Hydrol. Oceans Atmos.,* **24(8)** , 889–893.

Cullen, M.J.P. 1993 The Unified forecast/climate Model, *Meteorol. Mag.*, **122**, 81–94.

Dalezios, N.R. and Kouwen, N. 1990 Radar signal interpretation in warm season rainstorms. *Nordic Hydrology,* **21** , 47–64.

Duchon, C.E. and Essenberg, G.R. 2001 Comparative rainfall observations from pit and above-ground rain gauges with and without wind shields. *Water Resour. Res,* **37** , 3253–3263.

Fabry, F. 1993 Wind-profile estimation by conventional radars. *J. Appl. Meteor.,* **32** , 40–49.

Fabry, F. 1996 On the determination of scale ranges for precipitation fields. *J. Geophys. Res.,* **101(D8)** , 12819–12826.

Fabry, R., Austin, G.L. and Tees, D.	1992	The accuracy of rainfall estimates by radar as a function of range. *Q. J. R. Meteorol. Soc.,* **118** , 435–453.
Fabry, F., Bellon A., Duncan M.R. and Austin G.L.	1994	High-resolution rainfall measurements by radar for very small basins— the sampling problem reexamined. *J. Hydrol.,* **161** , 415–428.
Goddard, J.W.F. and Eastment, J.D. and Thurai, M.	1994	The Chilbolton advanced meteorological radar: a tool for multidisciplinary research, *Electron. & Commun. Eng. J.*, **6** , 77–86.
Harrold, T.W., English, E.J. and Nicholass, C.A.	1974	The accuracy of radar-derived rainfall measurements in hilly terrain. *Q. J. R. Meteorol. Soc.,* **100** , 331–350.
Joss, J. and Waldvogel, A.	1990	Precipitation measurement and hydrology, a review. In *Radar in Meteorology (Ed. D.Altas) American Meteorological Society* , 577–606.
Kitchen, M., Brown, R. and Davies, A.G.	1994	Real-time correction of weather radar data for the effects of bright band range and orographic growth in widespread precipitation. *Q. J. R. Meteorol. Soc.*, **120**, 1231–1254.
Locatelli, M., and Hobbs, P.V.	1974	Fall speeds and masses of solid precipitation particles. *J. Geophys. Res.*, **79** , 2185–2197.
Marshall, J.S.	1953	Precipitation trajectories and patterns. *J. Meteor.*, **10**, 25–29.
Mason, I.B.	2003	In *Forecast Verification. A practitioner's guide in Atmospheric Science, Chapter 3, Eds T. Joliffe and D.B. Stephenson, Wiley, 37–76.*
Mittermaier, M.P. and Illingworth, A.J.	2003	Comparison of model-derived and radar-observed freezing level heights: Implications for vertical reflectivity profile correction schemes. *Q. J. R. Meteorol. Soc.,* **128** , 83–96.
Panagi, P.M., Dicks, E.M., Hamer, G.L. and Nash, J.	2001	Preliminary results of the routine comparison of wind profiler data with the Meteorological Office Unified Model vertical wind profiles. *Phys. Chem. Earth. Part B Hydrol. Oceans Atmos.,* **26** , 187–191.
Sauvageot, H.	1992	*Radar Meteorology*, Artech House, 366pp.
Yuter, S.E. and Houze Jr., R.A.	1997	Measurements of raindrop size distributions over the Pacific warm pool and implications for Z-R relations. *J. Appl. Meteor.,* **36** , 847–867
Yuter, S.E. and Houze Jr., R.A.	2003	Microphysical modes of precipitation growth determined by S-band vertically pointing radar in orographic precipitation during MAP. *Q. J. R. Meteorol. Soc.,* **129**, 455-476